Wind-Tunnel Studies of F/A-18 Tail Buffet

B. H. K. Lee* and D. Brown*
National Research Council, Ottawa, Ontario, Canada

A wind-tunnel investigation of buffeting on the vertical fin of a rigid 6% model of the F/A-18 has been conducted in the Institute for Aerospace Research 5 × 5-ft Trisonic Blowdown Tunnel. Unsteady pressure measurements on the vertical fin were made by means of 24 fast response transducers on each surface. The vortex flow structure behind the fin was studied with the aid of a 49 pressure-sensor rake mounted on the model sting. In addition to measuring steady pitot pressure values to deduce pressure contours, unsteady pressure signals were obtained from 13 fast response transducers. Spectral analyses of the pressure fluctuations on the fin and in the vortical flow region behind the fin were performed to detect the presence of dominant oscillations during buffeting. The leading-edge extension was instrumented with pressure orifices and fast response transducers to study the flowfield beneath the roll-up vortex. The test was carried out with leading-edge extension fences on and off to note their effect on tail buffet loads.

Nomenclature

A_j = area of jth panel on vertical fin
A_T = total surface area of fin
C_M = aircraft steady pitching moment coefficient (moment axis 23.79 in. from nose)
C'_m = rms value of aircraft pitching moment coefficient
C_N = vertical fin normal force coefficient, positive outboard
C_P = steady pressure coefficient
C'_p = rms value of pressure coefficient
$\bar{c}$ = wing mean aerodynamic chord (8.29 in.)
$\bar{c}_f$ = vertical fin mean aerodynamic chord (5.03 in.)
c_f = local chord of fin
f = frequency
k = nondimensional frequency, $=f\bar{c}/U_\infty$
M = freestream Mach number
P_I = steady pressure on vertical fin inboard surface
P_O = steady pressure on vertical fin outboard surface
q = freestream dynamic pressure
$Re_{\bar{c}}$ = Reynolds number based on $\bar{c}$
U_∞ = freestream velocity
X, Y, Z = aircraft coordinate system measured from the nose
X_f, Y_f, Z_f = fin coordinate system
X_v, Y_v, Z_v = vortex rake coordinate system
α = angle of incidence

I. Introduction

MODERN combat aircraft must be capable of flying under conditions of separated flows in order to achieve high maneuverability. Aircraft structures under such conditions are subject to random aerodynamic loads arising from pressure fluctuations due to flow separations and/or impact of vortical flows on the structures. The loads are difficult to measure in flight, but a fair estimate can be predicted using wind-tunnel rigid model unsteady pressure measurements.[1-3] An example of this type of severe random aerodynamic loading is found in the F/A-18 vertical tail buffeting when the highly turbulent flows, resulting from bursting of the leading-edge extension (LEX) vortices, impact the vertical fins. The effect of buffet loads on structural integrity of the vertical fins is currently a major concern.

A number of studies on high angle-of-attack aerodynamics and the effect of the vortical flow on vertical tail buffeting have appeared in recent years.[4-8] These investigations focus mainly on the measurements of steady forces and pressures on the LEX,[4] laser light sheet measurements of the vortex structure,[4] as well as velocity flowfield surveys,[6] water-tunnel experiments on vortex burst phenomenon,[7] and some wind-tunnel model fin pressure measurements and vertical tail acceleration data from flight tests.[5]

Some results of an investigation of tail buffeting on a 6% rigid model of the F/A-18 carried out in the transonic test section of the 5 × 5-ft Trisonic Blowdown Wind Tunnel at the Institute for Aerospace Research (IAR) were given in an earlier paper[8] and more detailed findings are reported herein. One of the vertical fins was instrumented with fast response transducers on each surface to measure the unsteady pressures. The fin was also instrumented with strain gauges and an accelerometer for response measurements. The LEX was instrumented with pressure orifices and fast response transducers to provide information on the flowfield beneath the LEX vortex. The dynamics of the flowfield in the vicinity of the fin were also measured using a multitube vortex rake. All of the measurements were carried out with the LEX fences on and off so as to investigate the effect of modifying the vortical flow on tail buffet loads. During this wind-tunnel investigation, various values of M and q were used in the test program, but this paper gives results only for $M = 0.6$, $Re_{\bar{c}} = 3.38 \times 10^6$, $q = 3.95$ psi, and α from 0 to 35 deg.

II. Model and Instrumentation

The F/A-18 model was sting mounted from a vertically moving model support strut. A linkage mechanism provides a pitch angle change from −11 to 22 deg, and models may be rolled 360 deg. For the present measurements, the model was supported on an offset sting, with an 11-deg crank angle, which conferred an incidence range from 0 to 33 deg. Under aerodynamic load, an increment of 2 deg, due to sting and balance bending, is typically obtained.

Received May 3, 1990; presented as Paper 90-1432 at the AIAA 16th Aerodynamic Ground Testing Conference, Seattle, WA, June 18-20, 1990; revision received Dec. 17, 1990; accepted for publication Jan. 31, 1991.

*Senior Research Officer, Institute for Aerospace Research. Member AIAA.

The model consists of three major pieces, namely, an aluminum alloy nose section with integral strakes (LEX) equipped with removable fences and a single place canopy; a stainless steel center fuselage with integral wings; and a stainless steel rear fuselage. These parts are designed with close tolerance spigotted joints and are doweled and bolted together. The center fuselage is bored to accept a 1.5-in.-diam. Able Corp. sting balance. Leading- and trailing-edge flaps are fastened to the wings by simple bolted lap joints with dowel pins for accurate assemble. In the model tested, the leading- and trailing-edge flap deflections were set at 35 and 0 deg, respectively.

The vertical fins are fastened to a steel insert that in turn is bolted to the rear fuselage. The horizontal stabilators are made with integral spindles that are clamped in a fitting that is fixed in the rear fuselage. The stabilator angle was set at −9 deg for this investigation.

Through-flow air intakes and flow passages are provided with removable internal chokes. The flow passages terminate in D-shaped exits on each side of the support sting. Models of the AIM 9 missiles were fixed to the wingtips for the measurements.

The starboard side of the nose section was modified to incorporate 84 surface pressure orifices and four fast response EndevCo 8515B (50 psia) pressure transducers. The pressure orifices have a diameter of 0.02 in. and are distributed on the canopy centerline, upper fuselage side, two rows on the upper LEX, lower fuselage side, and on the lower LEX. The positions of the orifices on the upper surfaces are indicated in Fig. 1 and the coordinates are given in Ref. 8.

Orifice pressures were measured using five electronically scanned pressure modules that were contained in a cavity under the canopy. Each module contains 16 differential pressure transducers (±45 psi). Reference pressure from an accurately measured nitrogen source outside the wind tunnel was led via flexible Teflon tubing to the nose cavity.

The four fast reponse pressure transducer locations are also indicated in Fig. 1. These are installed beneath the LEX surface. Connection to the surface is by means of a very short (0.03 in.) passage of 0.020-in. diam., which gives a high-frequency response. The coordinate positions of the transducers are given in Ref. 8.

In this test, the standard starboard fin was replaced by an extensively instrumented fin, designed to measure dynamic pressures at 24 positions directly opposite to each other on each surface. In the construction, 48 EndevCo 8515B (50 psia) absolute pressure transducers are embedded under the surface and pressure is sensed via 0.02-in.-diam. passages, whose length varies from 0.014 to 0.025 in. In addition, four strain gauges are installed near the fin root at approximately half chord and an accelerometer (EndevCo Model 25, 1500g) is mounted 4.35 in. (75% span) from the root at $\frac{1}{3}$ local chord behind the leading edge. Positions of the pressure transducers are shown in Fig. 2 and numbered for later reference. Reference 8 gives their coordinates.

The vortex rake consists of a square array of 49 stagnation pressure measuring tubes supported, at 1-in. intervals, by two 6 × 6-in. frames. The rake was designed to achieve minimal flow blockage and yet be sufficiently rigid to withstand the high vibration levels from shed vortices of the model aircraft at high angles of incidence. Approximately 3 in. behind the support frames, the 0.095-in.-diam. tubes (0.071-in. bore) are gathered into a square bundle and housed in a square tube. This was clamped to the model support sting so as to place the face of the array a short distance (approximately 0.6 in.)

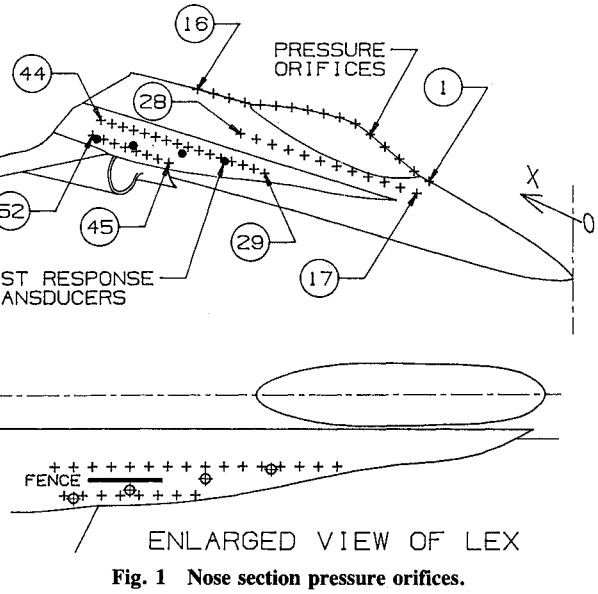

Fig. 1 Nose section pressure orifices.

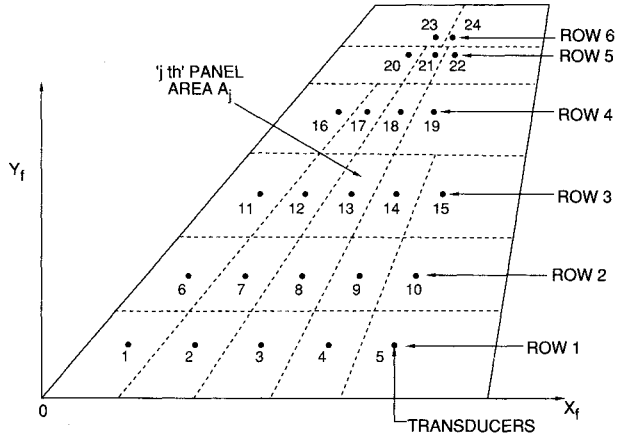

Fig. 2 Vertical fin pressure transducers.

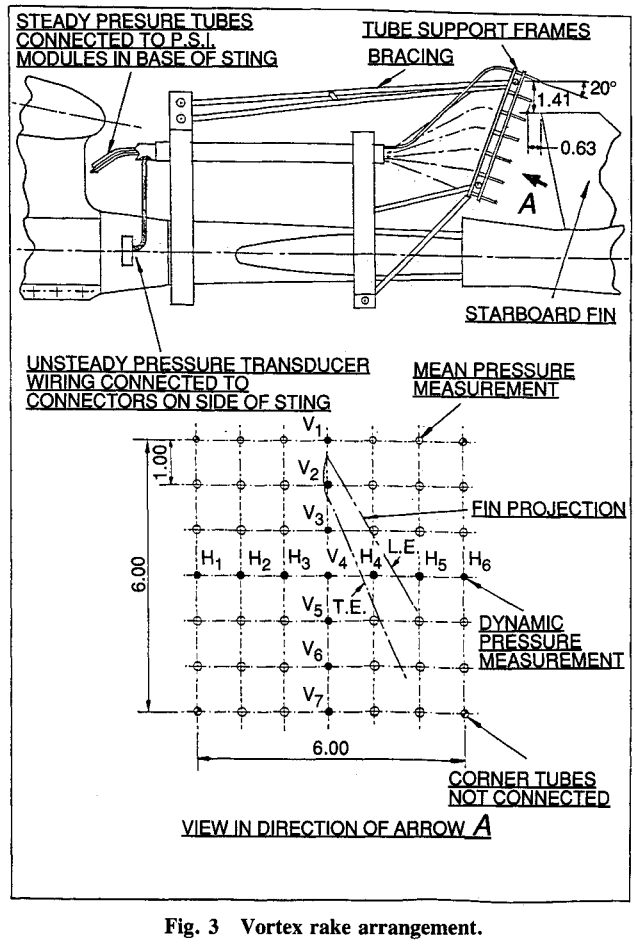

Fig. 3 Vortex rake arrangement.

behind the starboard fin and orientated at 20 deg to the aircraft model reference line, as indicated in Fig. 3.

Of the 45 active tubes, 13 (the corner tubes were not connected) were devoted to dynamic pressure measurements and the remainder to sensing steady pressures. These tubes are distributed on the vertical and horizontal centerlines of the array, as denoted in Fig. 3. High-frequency response was obtained by cementing $\frac{1}{8}$-in.-diam. Kulite differential pressure transducers (XCW-062, ±25 psi) just inside the tips of the 0.071-in. bore tubes.

The 36 steady pressure stagnation tubes were made by cementing short pieces of 0.070-in. o.d., 0.033-in. i.d. tubes inside the 0.071-in. bore tubing to form a 1-in.-long tip. The tips were connected to two 16-transducer electronically scanned pressure modules, which were also housed in the base of the sting, by 0.032-in. o.d., 0.02-in. i.d. stainless steel tubing cemented inside the tips of the rake tubes.

Internal chamfers of 40-deg included angle were machined in the ends of both dynamic and steady pressure tubes to reduce the directional sensitivity of the rake since it was required to operate over a 35-deg angle-of-incidence range. The rake was aligned with the freestream direction when the model incidence angle was 20 deg.

Accelerometers were installed at the upper corner of the rake closest to the model centerline to measure vibration levels. Boundary-layer transition trips were installed following the scheme laid down in Ref. 4. Rows of epoxy cylinders (0.045-in. diam. on 0.1-in. centers, 0.002-in. high) were applied 0.4 in. behind the leading edges of the LEX, wings, intakes, fins, and horizontal stabilators on both surfaces. In addition, a ring was applied around the nose, 0.4 in. behind the tip, and a longitudinal row was fixed on the underfuselage centerline from nose to the intakes' station.

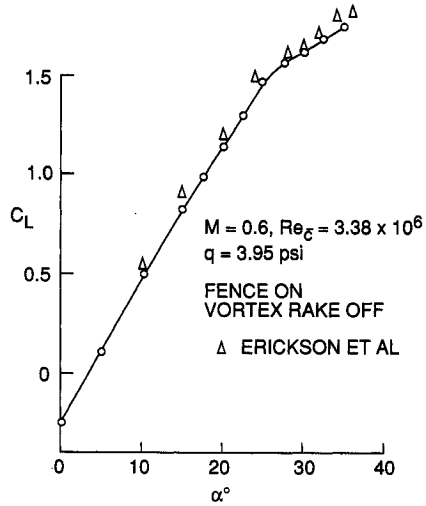

Fig. 4 C_L vs α.

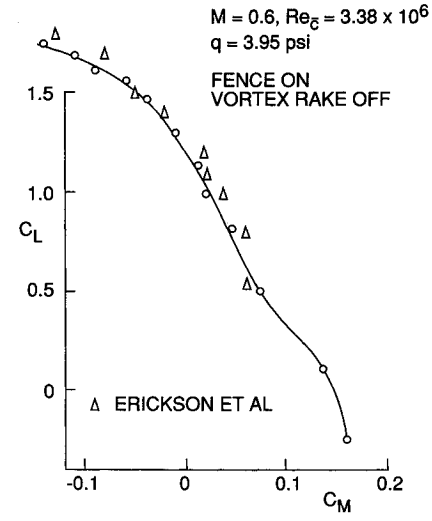

Fig. 5 C_L vs C_M.

III. Results and Discussion

A. Balance Measurements

Some steady C_L vs α and C_L vs C_M curves are given in Figs. 4 and 5. The presence of the LEX fence has little effect on the moment and lift measurements.[8] The results from Erickson et al.[4] are also included for comparison purposes. Their results were obtained from a 6% model in the David Taylor Research Center (DTRC) 7 × 10-ft transonic tunnel. The close agreement of the IAR results with those from a larger tunnel indicate that the wind-tunnel wall effects are probably

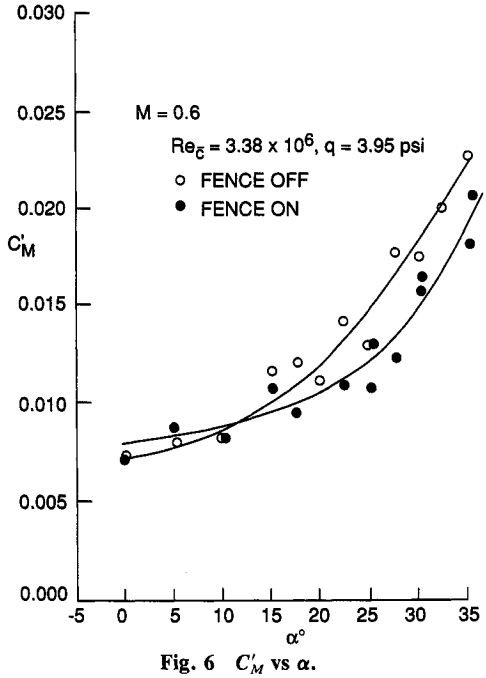

Fig. 6 C'_M vs α.

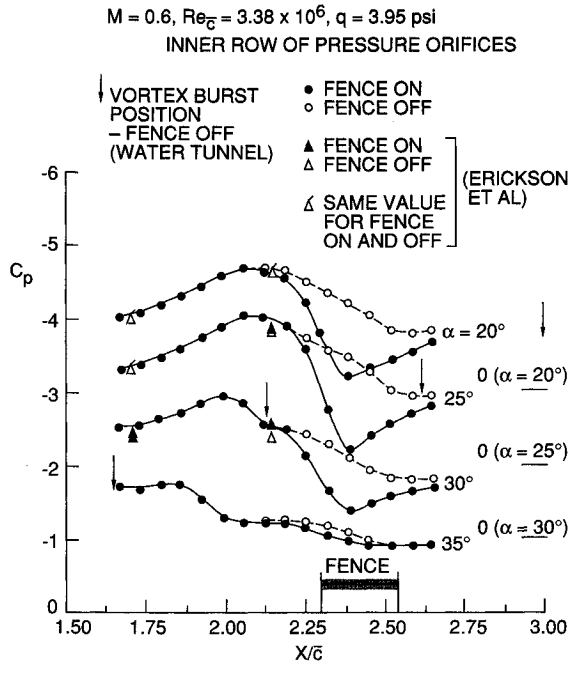

Fig. 7 C_p distributions on LEX upper surface.

not very significant in the present measurements. No wall interference corrections were applied to the present data.

Figure 6 shows the unsteady moment coefficient vs α. The scatter in the C'_M measurements is fairly large in the range of α between 15 and 25 deg. Video photography of the aircraft model during the wind-tunnel tests showed much larger vibratory motion at these values of α than at other angles of incidence. These large fluctuations are probably due to response from the horizontal tail buffeting. The LEX fence has little influence on C'_M until α is sufficiently large that the vortex burst is close to the tail. This angle is approximately 10 deg, which was observed from water-tunnel experiments.[8] The benefit of the LEX fence in reducing the pitching moment fluctuations is clearly demonstrated in this figure.

B. Leading-Edge Extension Upper Surface Pressures

Steady pressure measurements along the inner and outer rows of orifices on the LEX upper surface are shown in Figs. 7 and 8 for α = 20, 25, 30, and 35 deg. The scales are displaced one unit upward to avoid overlapping. Erickson et al.'s[4] results, which coincide with the orifice positions in the present test, are included for comparison purposes. The axial vortex burst positions with the fence off obtained from water-tunnel experiments[8] are also shown. At α = 35 deg, the vortex burst is ahead of the first measuring position on both rows of pres-

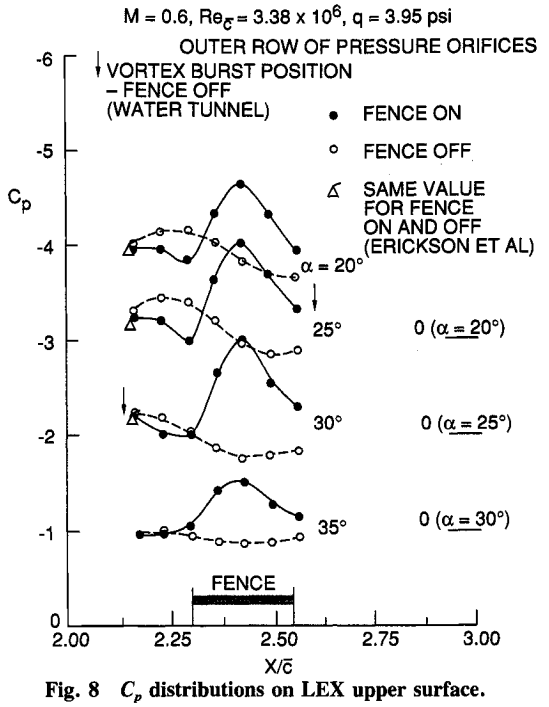

Fig. 8 C_p distributions on LEX upper surface.

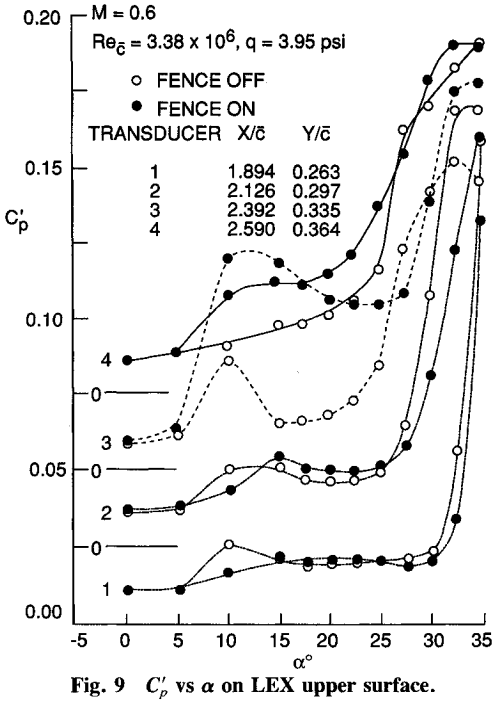

Fig. 9 C'_p vs α on LEX upper surface.

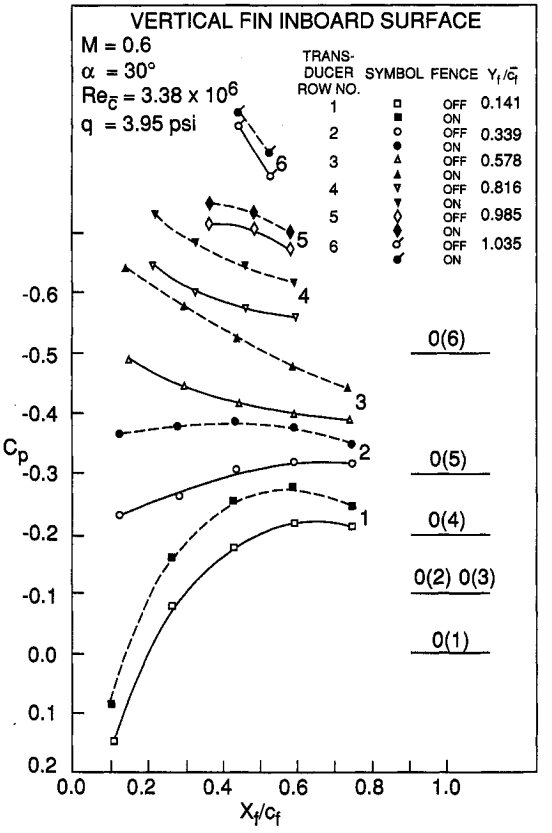

Fig. 10 C_p distributions on vertical fin inboard surface.

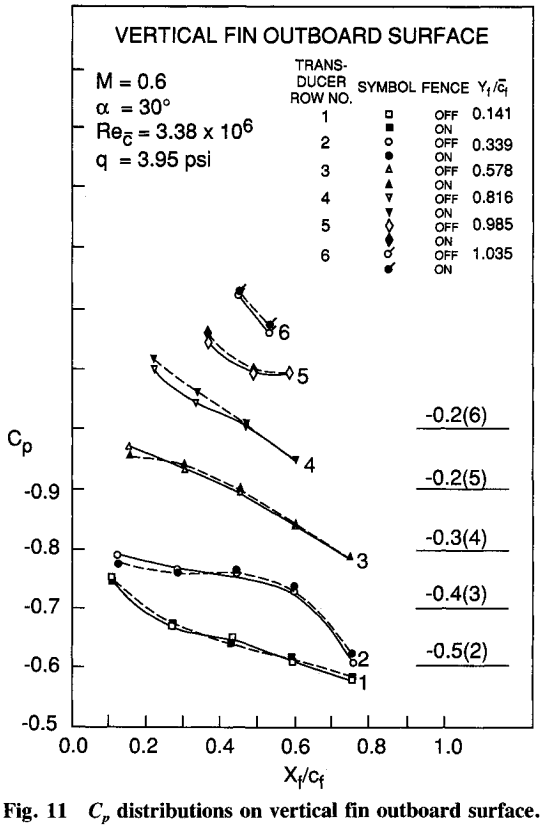

Fig. 11 C_p distributions on vertical fin outboard surface.

sure orifices and the fence has a small effect on the pressure measurements along the inner row of orifices, as shown in Fig. 7. Along the outer row of orifices there is a decrease in C_p with a minimum occurring near the middle of the fence (Fig. 8). Flow visualization in the vicinity of the fence using an oil dot technique showed the formation of a vortex outboard of the fence, which has a strong local influence on the pressure distribution.

At the lower values of α, Fig. 7 shows that the fence has a significant effect in altering the pressure distributions along the inner row of pressure orifices. The outer row shows the presence of a secondary vortex for all of the values of α considered.

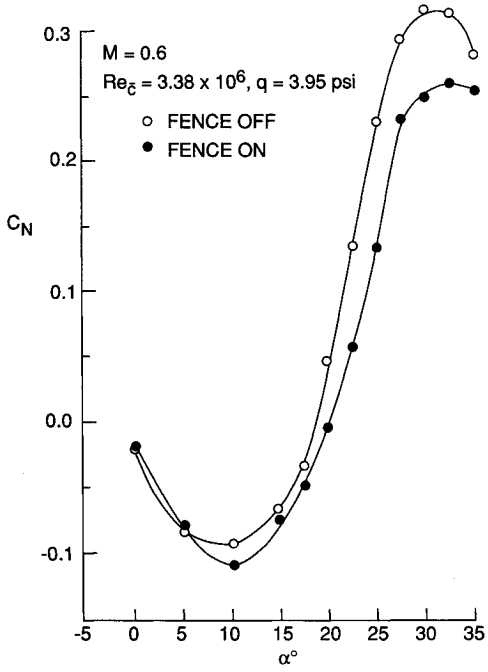

Fig. 12 Vertical fin C_N vs α.

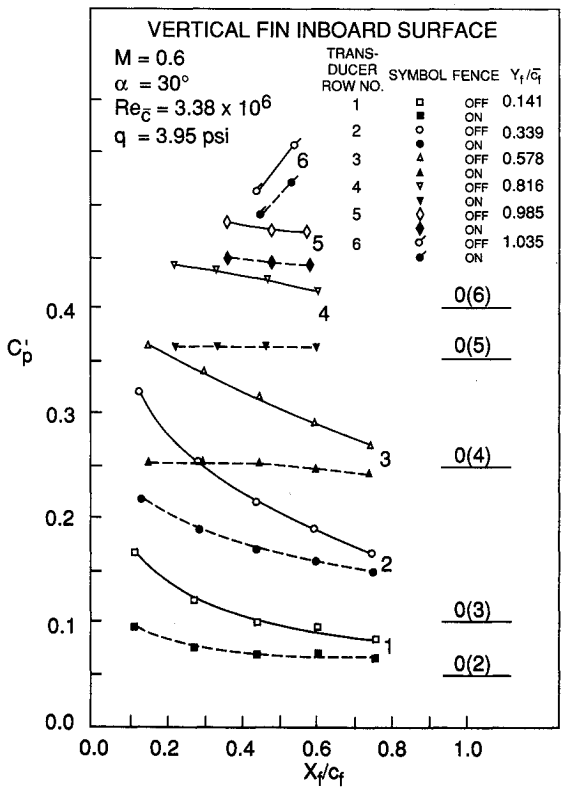

Fig. 13 C_p' distributions on vertical fin inboard surface.

The values of C_p' from the four fast response transducers are given in Fig. 9, where the curves are displaced 0.025 of a unit upward to avoid overlapping. At α = 10 deg, the first two transducers' measurements with the fence off show an increase in C_p' above those with the fence on.

At each transducer location, the value of α when C_p' starts to increase rapidly corresponds to the angle of incidence when the vortex burst is located near that transducer. For transducers 1 and 2, the effect of the fence is to lower the pressure fluctuations for values of α above those when the vortex has burst. A peak at α = 10 deg is also observed at the third transducer with the fence off. A large increase in C_p' is detected when the fence in on. This peak in C_p' is due to the vortex generated by the fence, which causes an increase in pressure fluctuations. At the fourth transducer, which is lo-

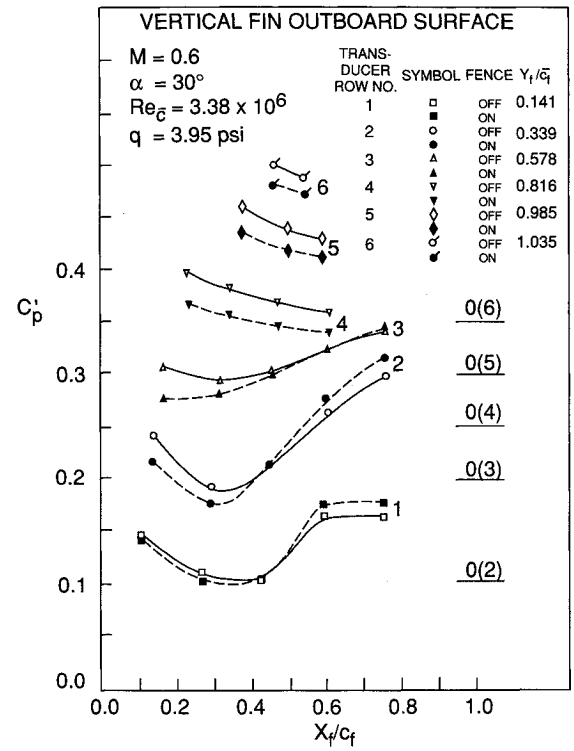

Fig. 14 C_p' distributions on vertical fin outboard surface.

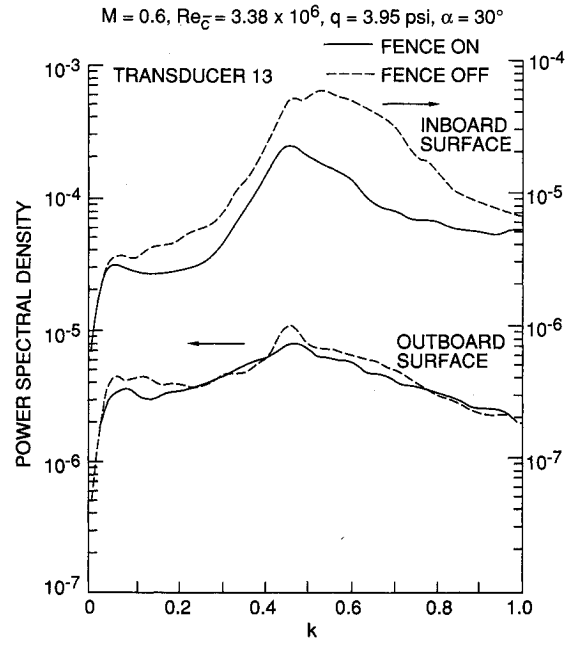

Fig. 15 Power spectral density of transducer 13 on vertical fin.

cated downstream of the fence trailing edge, the values of C_p' are consistently larger than those without the fence when α is between 5 and 25 deg.

C. Vertical Fin Pressures

The steady C_p distributions on the vertical fin inboard surface are shown in Fig. 10. The C_p curves for each row of transducers are displaced upward to avoid overlapping. The baseline is marked in the figure and the row number (see Fig. 2) of the transducers under consideration is given in parentheses. The effect of the fence is to decrease the steady-state pressures on the fin to values below those with the fence off. The difference is more pronounced in the middle of the fin than at the tip.

On the outboard surface of the vertical fin, the C_p distributions are given in Fig. 11. The fence has a small influence in modifying the steady pressures.

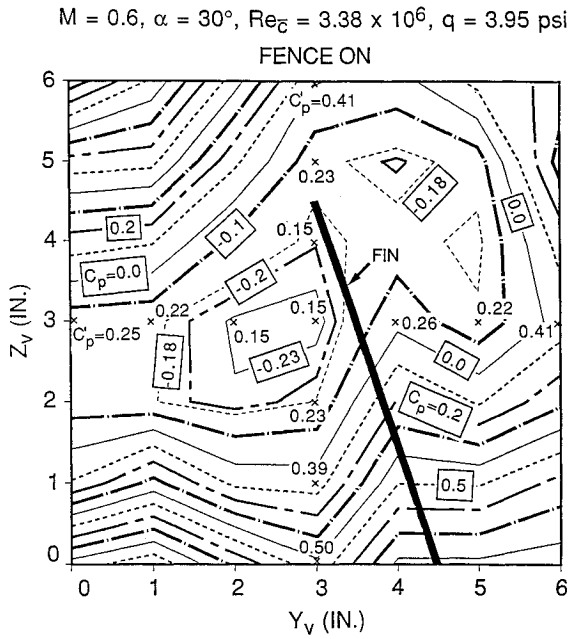

Fig. 16 Total pressure contours behind vertical fin with LEX fence on.

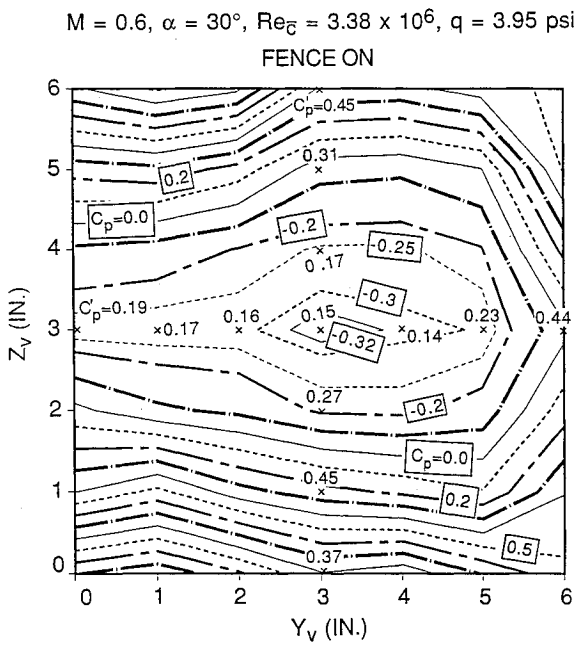

Fig. 17 Total pressure contours with tail section removed and LEX fence on.

Figure 12 shows the normal force C_N acting on the fin. This force is obtained by the following equation

$$C_N = \sum_{j=1}^{24} (p_{Ij} - p_{oj})A_j/qA_T \qquad (1)$$

and is positive outboard. The areas A_j of the panels are shown in Fig. 2. It is assumed that the pressure measured by each transducer is constant throughout the panel. For values of α up to about 20 deg, the fin force is negative but becomes much larger for $\alpha > 20$ deg. A maximum in C_N is observed at $\alpha \sim 30$ deg. The effect of the fence is to decrease fin normal force for $\alpha > 5$ deg.

The unsteady pressure fluctuations C_p' on the vertical fin inboard surface are shown in Fig. 13. The $C_p' = 0$ baseline is displaced upward for each row of transducers to avoid overlapping. The effect of the fence in lowering the pressure fluctuations is more pronounced near the fin leading edge and progressively diminishes toward the trailing edge for transducers rows 1, 2, and 3. As the tip of the fin is approached, the decrease in C_p' is more uniform along the fifth and sixth rows of transducers.

Figure 14 shows the pressure fluctuations on the outboard surface of the vertical fin. A much smaller decrease in pressure fluctuations is observed with the fence on than in the previous figure. In fact, for the first two rows of transducers, there is an increase in C_p' for $X_f > \sim 40\%$ of the local chord. The fence is more effective in lowering C_p' closer to the tip of the fin.

A typical plot of the power spectral density of the pressure coefficient is shown in Fig. 15 for transducer 13, which is located near the middle of the vertical fin. The Institute of Electrical and Electronic Engineers routine Periodgram Method for Power Spectrum Estimation (PMPSE)[9] is used to compute power spectral density. The data are digitized from FM tapes and have an equivalent sampling frequency of 80 kHz. The fast Fourier transform (FFT) block size used is 8192 and the resolution frequency is 9.76 Hz. Approximately 10 s of data was analyzed. At $\alpha = 30$ deg, a broad peak is observed on the inboard surface at a value of k between 0.45 and 0.5. A

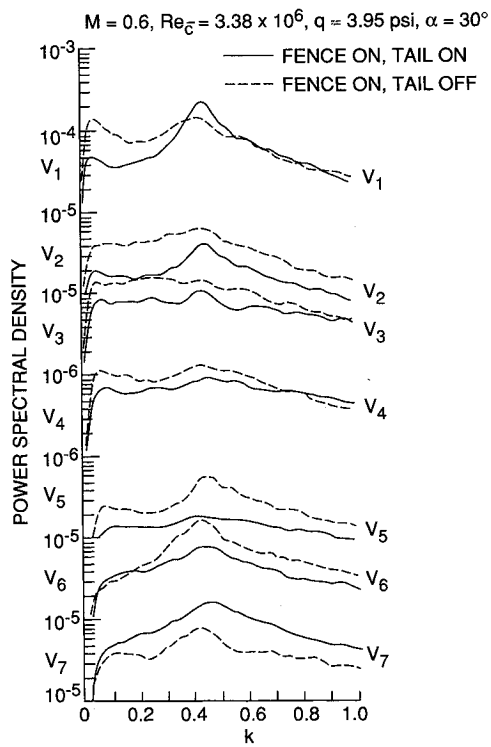

Fig. 18 Power spectral density of vortex rake vertical array of transducers.

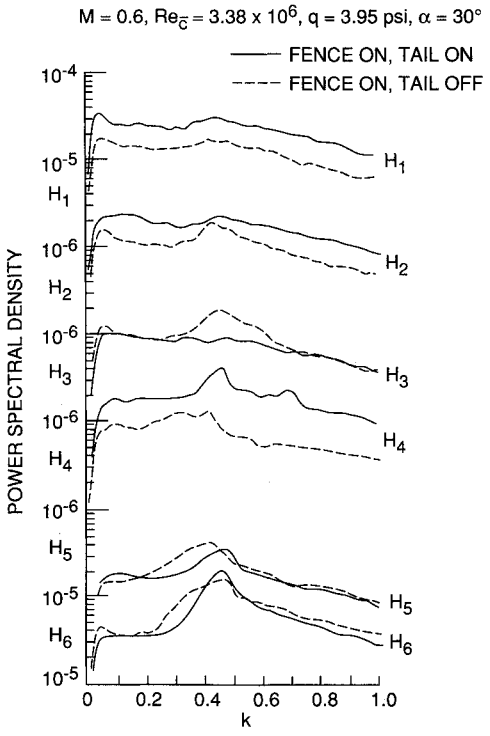

Fig. 19 Power spectral density of vortex rake horizontal array of transducers.

value close to this is also reported in Ref. 5. On the outboard surface, a distinct broad frequency peak is not observed at this location. However, the outer rows of transducers (rows 4–6) do exhibit this behavior. The fence has a greater effect on the inboard surface and this can be seen in the large reduction of the magnitude of the broad peak.

D. Vortical Flow Behind the Fin

The vortical flow's constant total pressure contour lines behind the vertical fin are shown in Fig. 16 at $\alpha = 30$ deg with the fence on. The center of the low-pressure region is located outboard of the vertical fin. Comparison with results in the absence of the fence shows that the constant pressure contour lines are more compressed in the vertical direction.[8] Inboard of the fin, a low-pressure region is also detected indicating the presence of a weaker secondary vortex system. The pressure fluctuations C_p' obtained from the midhorizontal and vertical rows of unsteady transducers are also included in this figure. The C_p' is smallest in the center of the vortex system and increases toward the edges of the rake. The magnitude of the pressure fluctuations increases more gradually outboard of the fin following the pattern of the elongation of the steady pressure contour lines.

To study the vortical flow without the interference of the vertical fins and horizontal stabilator, the tail section of the model aircraft was removed. The vortical flow structure is shown in Fig. 17 with the fence on. Again, the presence of the fence results in a compression of the steady pressure contour lines.[8] The lowest C_p' is also located in the center of the low-pressure region. Further studies in correlating the pressures in the vortical flow with those on fin are in progress.

Figure 18 shows the power spectral density plots for the vertical array of transducers on the vortex rake with the LEX fence on and the tail section on and off. The broad peak at k between 0.45 and 0.5 is observed in both cases. With the tail on, the peak is noticeable above and beneath the core of the low-pressure region located near the center of the rake. With the tail off, the peak is observed mainly near the lower portion of the vortex system.

The power spectral density plots along the horizontal array of transducers (Fig. 19) show stronger and more distinct peaks on the inboard side of the vortex.

IV. Conclusions

1) The LEX fence has a small influence on the steady balance measurements, such as lift and pitching moment. Fluctuating quantities, however, are reduced with the fence on.

2) At high α above 25 deg, there is a large increase in the unsteady pressure fluctuations on the upper surface of the LEX.

3) There are large reductions in steady and unsteady pressures on the vertical fin inboard surface with the LEX fence on at $\alpha = 30$ deg. The fence has a lesser effect on the outboard surface. Steady normal force calculated from pressure measurements show a significant decrease with the fence on.

4) At high α, total pressure contours of the vortical flow behind the vertical fins show the center of the low-pressure region to be located outboard of the fins. With the fence on, the contour lines are more compressed in the vertical direction.

5) Spectral analyses of the vertical fin and vortical flow pressures show a broad peak at a value of k between 0.45 and 0.5.

Acknowledgments

This work was supported in part by the Department of National Defence. F. A. Ellis and N. Tang provided technical assistance.

References

[1]Mullans, R. E., and Lemley, C. E., "Buffet Dynamic Loads During Transonic Maneuvers," Air Force Flight Dynamics Laboratory, Wright-Patterson Air Force Base, Ohio, TR-72-46, Sept. 1972.

[2]Lee, B. H. K., "A Method for Predicting Wing Response to Buffet Loads," *Journal of Aircraft*, Vol. 21, No. 1, 1984, pp. 85–87.

[3]Lan, C. E., and Lee, I. G., "Investigation of Empennage Buffeting," NASA CR-179426, Jan. 1987.

[4]Erickson, G. E., Hall, R. M., Banks, D. W., Del Frate, J. H., Schreiner, J. A., Hanley, R. J., and Pulley, C. T., "Experimental Investigation of the F/A-18 Vortex Flows at Subsonic Through Transonic Speeds, Invited Paper," AIAA Paper 89-2222, July 31–August 2, 1989.

[5]Zimmerman, N. H., Ferman, M. A., and Yurkovich, R. N., "Prediction of Tail Buffet loads for Design Application," AIAA Paper 89-1378, April 1989.

[6]Sellers, W. L., III, Meyers, J. F., and Hepner, T. E., "LDV Surveys Over a Fighter Model at Moderate to High Angles of Attack," Society of Automotive Engineers, Aerospace Technology Conference and Exposition, Anaheim, California, TP-88-1448, Oct. 1988.

[7]Wentz, W. H., Jr., "Vortex-Fin Interaction on a Fighter Aircraft," AIAA Paper 87-2474, Aug. 1987.

[8]Lee, B. H. K., Brown, D., Zgela, M., and Poirel, D., "Wind Tunnel Investigation and Flight Tests of Tail Buffet on the CF-18 Aircraft," Paper 1, AGARD Conference Proceedings No. 483, 1990.

[9]Rabiner, L. R., Schafer, R. W., and Dlugos, D., "Periodgram Method for Power Spectrum Estimation," *Programs for Digital Signal Processing*, edited by the Digital Signal Processing Committee, IEEE Acoustics, Speech and Signal Processing Society, IEEE Press, New York, 1979, Chap. 2.1.